

White Matter and Subcortical Gray Matter Microstructural Integrity in Mesial Temporal Lobe Epilepsy: A Combined Diffusion Tensor and Kurtosis Imaging Study

Hossein Sanjari Moghaddam ^{1,2}, Roya Sharifpour ^{3,4}, Amir Hossein Rasouli ^{5,6}, Neda Mohammadi Mobarakeh ^{3,4}, Sohrab Hashemi-Fesharaki ⁷, Jafar Mehvari Habibabadi ⁸, Mohammad-Reza Nazem-Zadeh ^{3,4,*} 

¹ School of Medicine, Tehran University of Medical Sciences, Tehran, Iran

² Student's Scientific Research Center, Tehran University of Medical Sciences, Tehran, Iran

³ Department of Medical Physics and Biomedical Engineering, School of Medicine, Tehran University of Medical Sciences, Tehran, Iran

⁴ Research Center for Molecular and Cellular Imaging, Advanced Medical Technologies and Equipment Institute, Tehran University of Medical Sciences, Tehran, Iran

⁵ Movement Control and Neuroplasticity Research Group, Department of Movement Sciences, Group Biomedical Sciences, KU Leuven, Leuven, Belgium

⁶ Leuven Brain Institute, KU Leuven, Leuven, Belgium

⁷ Pars Advanced and Minimally Invasive Medical Manners Research Center, Pars Hospital, Tehran, Iran

⁸ Neuroscience Research Center, Research Centers, Isfahan University of Medical Sciences, Isfahan, Iran

*Corresponding Author: Mohammad-Reza Nazem-Zadeh
Email: m_nazemzadeh@yahoo.com

Received: 20 January 2020 / Accepted: 24 March 2020

Abstract

Purpose: The present study aimed to assess structural asymmetry in patients with mesial Temporal Lobe Epilepsy (mTLE) in the diffusion properties of brain white matter and subcortical gray matter tracts using Diffusion Tensor Imaging (DTI) and Diffusion Kurtosis Imaging (DKI). We considered a lower order DTI measure, Fractional Anisotropy (FA), and a higher-order DKI measure, Kurtosis Anisotropy (KA), as quantitative measures of the white matter diffusion properties in facing mTLE. We also made a comparison between these two measures in terms of the sensitivity to capture microstructural changes in concordance with TLE.

Materials and Methods: Thirty-two subjects with mTLE participated in this study. All the cases underwent multi-shell diffusion MRI acquisition. The subjects were grouped according to their epileptogenic side of the brain (19 Left-sided and 13 Right-sided TLE). Each group were analyzed separately using FSL package, then laterality analysis based on Tract-Based Spatial Statistics (TBSS) was performed on FA and KA images. After each analysis the left side of the patients' brain was flipped and subtracted from the right side of the patients's brain, and a voxel-wise z-score comparison was applied to find the significantly different areas.

Results: The results showed a considerable laterality effect on the temporal lobe white matters both in FA and KA, more emphasized in patients with Right-sided mTLE.

Conclusion: It can be concluded that these two measures, even though extracted from skeletonized images, can serve as decent biomarkers of laterality in case of mTLE, when the conventional MRI fails to capture the laterality.

Keywords: Microstructural Integrity; Mesial Temporal Lobe Epilepsy; Laterality; Epileptogenic Side; Diffusion Tensor Imaging; Diffusion Kurtosis Imaging.

1. Introduction

The brain functional and structural laterality -the normalized variation of a brain functional or structural index between left and right hemispheres- has been of the main questions in brain studies. The most evident macrostructural interhemispheric asymmetries are larger right frontal region and larger left occipital petalias and the planum temporale in healthy cases. Regarding the functional lateralization, it has been consistently reported that language processes are mainly handled by the left hemisphere and spatial cognitive functions are processed in the right hemisphere [1-4]. Although, the healthy brain is accompanied by some inherent asymmetries, some neurological disorders, such as epilepsy [5] and autism [6] are associated with aberrant interhemispheric asymmetries. Epilepsy is a common neurological disorder in which brain's nerve cells fire electrical impulses at a rate of up to four times higher than normal. This abnormal discharging of nerve cells in the brain is known as a seizure. A pattern of repeated seizures is referred to as epilepsy. Mesial Temporal Lobe Epilepsy (mTLE) is one the most common types of epilepsy and is defined by unprovoked focal seizures rising from the inner (medial) aspect of the temporal lobe [7]. A plethora of evidence has shown that mTLE is associated with aberrant functional and microstructural alterations, which lead to deficits in several cognitive functions [8-11]. Most of mTLE patients eventually become unresponsive to pharmacological treatment, which necessitates the surgical resection of the seizure focus, which is lateralized to the right or left temporal lobe [12]. Thus, reliable lateralization of seizure focus is necessary prior to the surgery.

Diffusion Tensor Imaging (DTI) is an MRI method, which is based on the diffusion of water molecules in three directions of the space. DTI has been vastly used for the assessment of white matter microstructure of the brain in many neurological disorders [13, 14]. The primary parameter derived from DTI is known as Fractional Anisotropy (FA), which quantifies the directionality of water anisotropic diffusion. Although FA has been generally attributed to white matter "integrity", the exact biological interpretation of FA is elusive. Numerous studies have shown that both left

and right mTLE is associated with alteration if the values of DTI_FA [15-17]. Of significant importance, DTI is based on the assumption that displacement distribution of water diffusion is Gaussian [18], which is not the case in biological settings where water diffusion is hindered by cell membranes and protein accumulations [19]. As a corollary, Diffusion Kurtosis Imaging (DKI) has been introduced to describe non-Gaussian diffusion using the kurtosis of the displacement distribution [20, 21]. The main measure derived from DKI is known as Kurtosis Fractional Anisotropy (KFA). Compared to conventional DTI, the measures of DKI have exhibited enhanced sensitivity and specificity in identification of white matter abnormalities in different brain disorders [22-26].

In this bimodal study, we have investigated two groups of left and right mTLE patients with simultaneous use of DTI and DKI for two main objectives; primarily, to interrogate the pattern of white matter microstructural asymmetries in left and right mTLE patients, and secondarily, to qualitatively compare the information provided by DTI and DKI regarding the interhemispheric asymmetries in left and right mTLE patients.

2. Materials and Methods

2.1. Human Subjects

This research study was approved by the Institutional Review Board of Iran University of Medical Sciences and involved 32 unilateral patients with left or right mTLE who were the candidates for surgical resection of a medial temporal structure. Thirteen cases were right-mTLE (17-36 years old: 26.8 ± 6.2 (mean \pm SD)) and nineteen cases were left-mTLE (17-54 years old: 31.9 ± 8.2 (mean \pm SD)).

The side of epileptogenicity was consented and established in a multidisciplinary decision-making session before the surgery. It was blinded during all processing.

2.2. Image Acquisition

All the cases underwent multi-shell Diffusion MRI acquisition using a 64-channel phased array head coil

on 3-Tesla scanner (Siemens Prisma, Erlangen, Germany) with software version “Syngo MR E11” at Iranian National Brain Mapping Laboratory (NMBL).

Structural MRI for clinical diagnosis was acquired using a standardized protocol, including transverse T1 weighted images using MPRAGE protocol with the following imaging parameters: TR = 1840 ms, TI=900 ms, TE = 2.43ms, flip angle = 8°, matrix = 224×224, in-plane resolution=1.0×1.0 mm², slice thickness = 1.0 mm, pixel bandwidth = 250 Hz/pixel.

Multishell DTI images (b-values of 1000 and 2000 s/mm²) in 64 diffusion gradient directions on each shell along with a set of null images (b-value of 0 s/mm²) were acquired using Echo Planar Imaging (EPI) on the same machine in anterior to posterior phase direction with the following imaging parameters: TR = 9600 ms, TE = 92 ms, flip angle = 90°, matrix = 110 × 110, in-plane resolution = 2.0×2.0 mm², slice thickness = 2.0 mm, pixel bandwidth = 1420 Hz/pixel.

Two non-diffusion weighted (b=0) volumes were acquired with two opposite phase-encoding directions to perform distortion correction.

The main phase encoding direction was Anterior to Posterior (AP) and b=0 image with AP direction was extracted from the main acquisition. The other b=0 image with reversed phase encoding direction (PA) was acquired separately.

2.3. Pre-Processing

The image data was undertaken through some preprocessing steps, including motion correction, eddy current correction, followed by a two-step registration protocol. First, each DWI volume was registered to its own T1 space, then, using the transformation registering the subjects’ T1 to MNI space, all DWI volumes were transformed into standard MNI space.

2.4. Tensor Fitting and DKI Analysis

After preprocessing, using ExploreDTI (v4.8.6) package in Matlab 2015b, tensor fitting was performed to all of the subjects and index maps of FA. DKI fitting was also performed according to the following

formula, and Kurtosis Anisotropy (KA) map was calculated.

$$1n[S(b)/S_0] = -bD_{app} \quad (1)$$

$$1n[S(b)/S_0] = -bD_{app} + 1/6 b^2 D_{app}^2 K_{app} \quad (2)$$

where D_{app} and K_{app} are the apparent diffusion and kurtosis coefficients, respectively, along a given diffusion direction with diffusion-weighted signal $S(b)$ along that direction with a certain b-value. S_0 is the non-diffusion weighted signal. From this equation KA is calculated in the following Equation:

$$KA = \frac{\beta}{\sqrt{2}} * \frac{\sqrt{(K1-\bar{K})^2 + (K2-\bar{K})^2 + (K3-\bar{K})^2}}{\sqrt{K1^2 + K2^2 + K3^2}} \quad (3)$$

where $\bar{K} = (K1 + K2 + K3)/3$.

After passing all of the subjects through the mentioned analysis procedure and extracting the index maps, the data became ready for voxel-wise group analysis.

2.5. Group Analysis

For the voxel-wise group analysis, we used the FSL software library Functional Magnetic Resonance Imaging of the Brain (FMRIB; <http://www.fmrib.ox.ac.uk/fsl> [27]. Tract-Based Spatial Statistics (TBSS) is also a standard protocol for such a voxel-wise group analysis [28, 29]. In our proposed algorithm, every single index map (FA and KA, separately) underwent a skeletonization to achieve white matter areas and the core of each route. Then, using a non-linear registration algorithm all maps were transformed into a common MNI space. Hence, all white matter tracks and the maps became matched to those of the atlas. The goal was to detect areas with high degree of laterality between left and right hemispheres. For this purpose, the left side of the brains flipped and overlaid on the opposite side and the normalized difference (Asymmetry Index) between them was calculated for every voxel as follows:

$$AI = (Right - Left) / ((Right + Left) / 2)$$

Then, the mean ($Mean_{AI}$) and Standard Deviation (SD_{AI}) of the whole set of AI values were calculated and z-score value (Z_{AI}) was derived for every voxel as:

$$Z_{AI} = (AI - Mean_{AI}) / SD_{AI}$$

Assuming a normal distribution of values, voxels with $|Z_{AI}| \geq 1.64$ corresponding to $p\text{-value} < 0.05$ were considered to have significant difference between hemispheres.

3. Results

3.1. TBSS Analysis of DTI_FA

As detailed in Table 1, TBSS analysis of DTI_FA interhemispheric asymmetries demonstrated multiple significant WM clusters in both left and right mTLE patients. Although the number of DTI_FA interhemispheric asymmetries clusters were higher in the left compared to right mTLE patients, patients with left mTLE showed decreased volume of DTI_FA asymmetries compared to patients with right mTLE.

In left mTLE patients five significant asymmetric clusters were identified: First cluster of 10586 voxels involving the underlying WM/subcortical GM of thalamus, midbrain, hippocampus and parahippocampal gyrus, insula, amygdala, and caudate; second cluster of 4115 voxels, mainly localized in brainstem and cerebellum involving the underlying WM/subcortical GM of pons, cerebellum

anterior lobe, and midbrain; third and fourth clusters of 2262 and 1286 voxels, respectively, localized in frontal lobe containing the underlying WM/subcortical GM of superior frontal gyrus and medial frontal gyrus; fifth cluster of 853 voxels, main localization in occipital lobe comprising the underlying WM of cuneus and precuneus (Figure 1; $p < 0.05$).

In right mTLE patients, two significant clusters of asymmetric DTI_FA were detected: First cluster of 23401 voxels mainly localized in temporal lobe encompassing the underlying WM/subcortical GM of multiple regions, including inferior, superior, and medial temporal gyri, thalamus, fusiform gyrus, limbic lobe, hippocampus and parahippocampal gyrus, insula, midbrain and brainstem, putamen, caudate, and amygdala; second cluster of 3671 voxels, main localization in frontal lobe involving the underlying WM/subcortical GM of precentral gyrus, inferior parietal lobule, postcentral gyrus, and inferior frontal gyrus (Figure 2, $p < 0.05$).

3.2. TBSS Analysis of DKI_KFA

TBSS analysis of DKI_KFA interhemispheric asymmetries identified several significant WM clusters in both left and right mTLE patients (Table 2).

Table 1. TBSS analysis of DTI_FA interhemispheric asymmetries demonstrated multiple significant WM clusters in both left and right mTLE patients. Note that patients with left mTLE showed decreased volume of DTI_FA asymmetries compared to patients with right mTLE

TLE laterality	Cluster main localization	Number of voxels	Peak MNI coordinate	Underlying WM/ Subcortical GM
Left TLE	Thalamus, Midbrain and Temporal lobe	10586	-12 -12 -13	Thalamus, Midbrain, Hippocampus and PHG, Insula, Amygdala, and Caudate
	Brainstem and Cerebellum	4115	-19 -36 -36	Pons, Cerebellum Anterior Lobe, and Midbrain
	Frontal lobe	2262	-26 -1 32	Frontal lobe
	Frontal lobe	1286	-19 50 12	SFG and MFG
	Occipital lobe	853	-25 -69 14	Cuneus and Precuneus
Right TLE	Temporal lobe	23401	-25 -22 1	ITG, STG, MTG, Thalamus, FG, Limbic lobe, Hippocampus and PHG, Insula, Midbrain and Brainstem, Putamen, GP, Caudate, and Amygdala
	Frontal and Parietal lobes	3671	-38 -16 28	PreCG, IPL, PostCG, and IFO

Table note: IPL: Inferior Parietal Lobule; PreCG: Precentral Gyrus; PostCG: Postcentral Gyrus; IFG: Inferior Frontal Gyrus; IFO: Inferior Frontal Operculum; ITG/MTG/STG: Inferior/Middle/Superior Temporal Gyrus; FG: Fusiform Gyrus, PHG: Parahippocampal Gyrus; GP: Globus Pallidus; SFG/MFG: Superior/Middle Frontal Gyrus

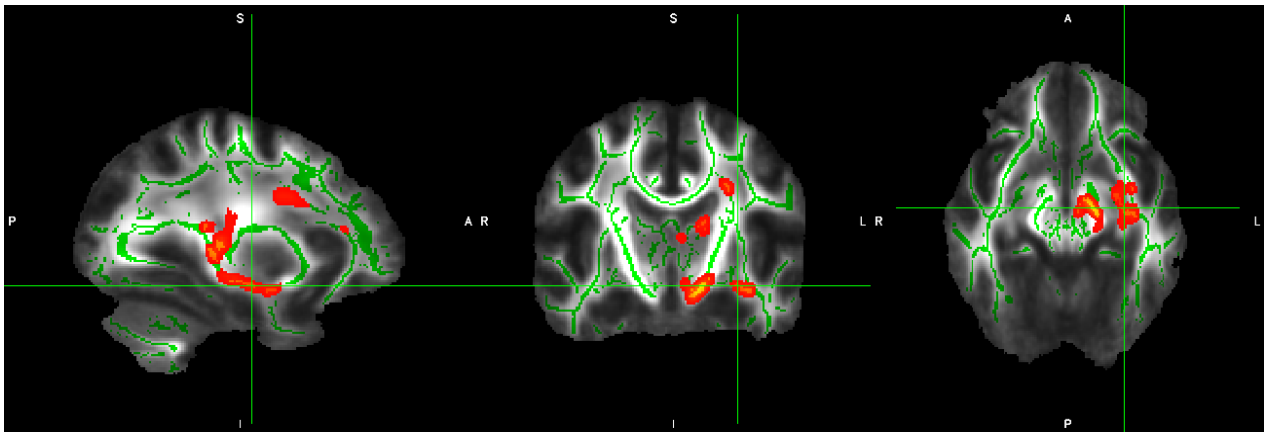


Figure 1. The average map of FA and TBSS for left mTLE patients with five significant asymmetric clusters involving the underlying WM/subcortical GM of the thalamus, midbrain, hippocampus and parahippocampal gyrus, insula, amygdala, caudate, pons, brainstem, cerebellum anterior lobe and midbrain, superior and medial frontal gyri, cuneus and precuneus. Note that the left side of the brains was flipped and overlaid on the right side and the normalized difference between them was calculated and visualized

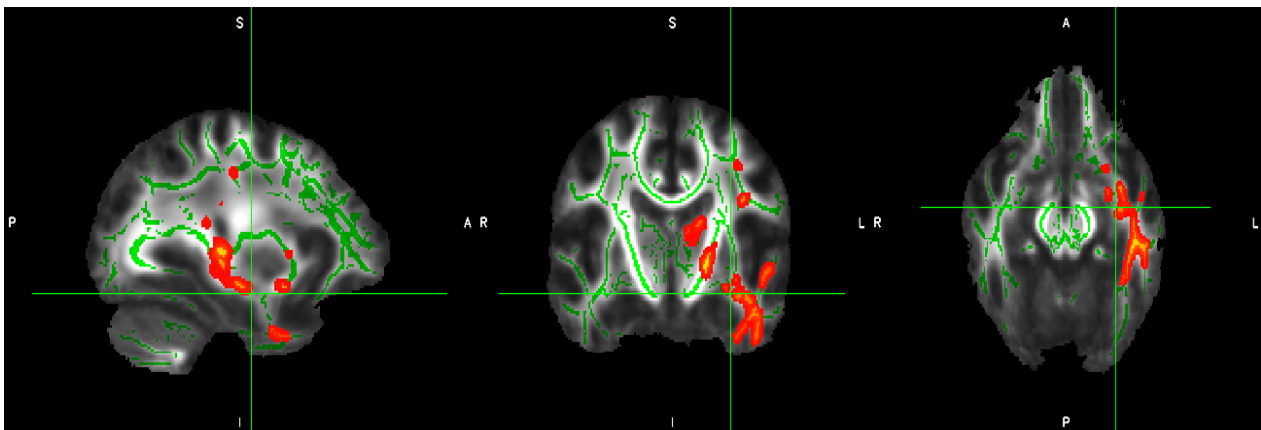


Figure 2. The average map of FA and TBSS for right mTLE patients with two significant asymmetric clusters involving the underlying WM/subcortical GM of inferior, superior, and medial temporal gyri, thalamus, fusiform gyrus, limbic lobe, hippocampus and parahippocampal gyrus, insula, midbrain and brainstem, putamen, caudate, and amygdala, precentral gyrus, inferior parietal lobule, postcentral gyrus, and inferior frontal gyrus. Note that the left side of the brains was flipped and overlaid on the right side and the normalized difference between them was calculated

Again, compared to right mTLE patients, patients with left mTLE showed lower volume of DKI_KFA asymmetries.

In left mTLE patients, three relatively small clusters of asymmetric KFA were spotted. The clusters were 2125, 541, and 511 voxels large, and all were mainly localized in frontal lobe encompassing the underlying WM/subcortical GM of inferior parietal lobule, precentral and postcentral gyri, and opercular part of inferior frontal gyrus (Figure 3, $p < 0.05$).

In right mTLE patients, three significant clusters of asymmetric DKI_KFA were identified: First cluster of

20927 voxels, main localization in temporal lobe involving the underlying WM/subcortical GM of numerous regions, including inferior, middle, and superior temporal gyri, inferior parietal lobule, hippocampus and parahippocampal gyrus, opercular part of inferior frontal gyrus, supramarginal gyrus, insula, thalamus, precentral and postcentral gyri, angular gyrus, fusiform gyrus, and putamen; second cluster of 1160 voxels, main localization in limbic system involving the cingulum and underlying WM of cingulate gyrus; third cluster of 614 voxels mainly localized in frontal lobe involving underlying WM of insula (Figure 4, $p < 0.05$).

Table 2. TBSS analysis of DKI_FA (KFA) interhemispheric asymmetries demonstrated multiple significant WM clusters in both left and right mTLE patients. Note that patients with left mTLE showed decreased volume of DKI_FA asymmetries compared to patients with right mTLE

TLE laterality	Cluster main localization	Number of voxels	Peak MNI coordinate	Underlying WM/Subcortical GM of
Left TLE	Frontal and Parietal lobes	2125	-37 -16 29	IPL, PostCG, and PreCG
	Frontal lobe	541	-26 -5 34	Frontal lobe
	Frontal lobe	510	-37 3 22	IFO
Right TLE	Temporal lobe and to some extent in Frontal and Parietal lobes	20927	-23 -21 -2	ITG, MTG, STG, IPL, Hippocampus and PHG, IFO, SMG, Insula, Thalamus, PreCG, PostCG, AG, FG, and Putamen
	Limbic system	1160	-8 -5 34	Cingulum and CG
	Frontal lobe	614	-23 23 7	Insula

Table note: IPL: Inferior Parietal Lobule; PreCG: Precentral Gyrus; PostCG: Postcentral Gyrus; IFG: Inferior Frontal Gyrus; IFO: Inferior Frontal Operculum; ITG/MTG/STG: Inferior/Middle/Superior Temporal Gyrus; FG: Fusiform Gyrus, PHG: Parahippocampal Gyrus; GP: Globus Pallidus; SFG/MFG: Superior/Middle Frontal Gyrus; SMG: Supramarginal Gyrus; AG: Angular Gyrus; CG: Cingulate Gyrus

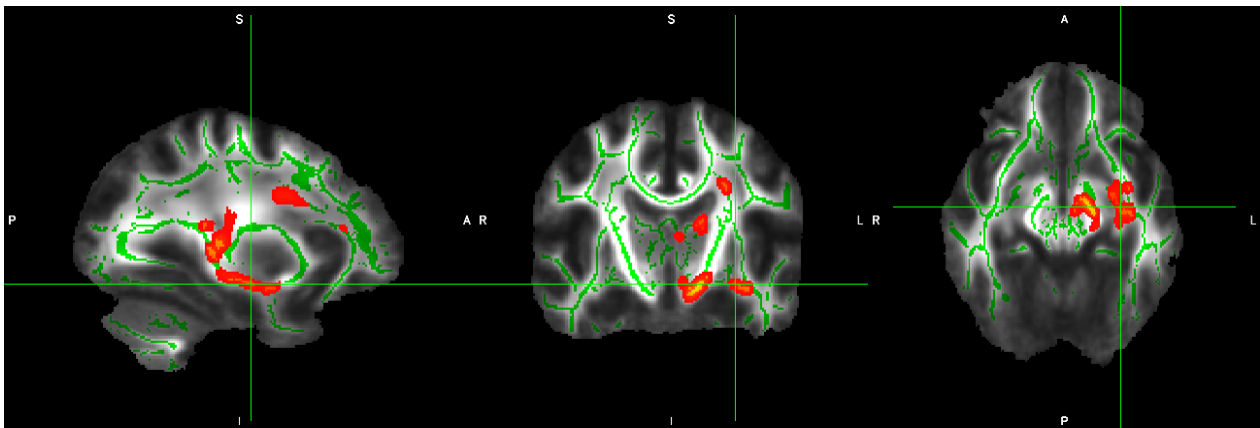


Figure 3. The average map of KFA and TBSS for left mTLE patients with three significant asymmetric clusters involving the underlying WM/subcortical GM of the inferior parietal lobule, precentral and postcentral gyri and opercular part of inferior frontal gyrus. Note that the left side of the brains was flipped and overlaid on the right side and the normalized difference between them was calculated

4. Discussion

Over recent years, several DTI studies have scrutinized the white matter structural abnormalities in patients with left and right mTLE [7, 30-34]. However, the pattern of white matter microstructural asymmetries in left and right mTLE patients remain noticeably unaddressed. Newly developed imaging techniques, such as DKI could provide more detailed and sensitive information regarding the asymmetry of white matter microstructure and thus the lateralization of mTLE [35].

Our findings from DTI showed that more extended extra-temporal asymmetries in left MLTE patients and

more temporal asymmetries in right mTLE patients. Besides, left mTLE compared to right mTLE patients displayed slightly diminished interhemispheric asymmetries. The same pattern was revealed by DKI (extra-temporal asymmetries in left and temporal asymmetries in right mTLE), however, left mTLE patients showed considerable reduction of interhemispheric asymmetries compared with patients with right mTLE. Collectively, these findings suggest that left mTLE is associated with more decreased interhemispheric asymmetries compared to right mTLE. Even though, as we did not include a group of healthy controls, it could not be concluded whether the existence or reduction of interhemispheric asymmetries is in favor of disease progression. The

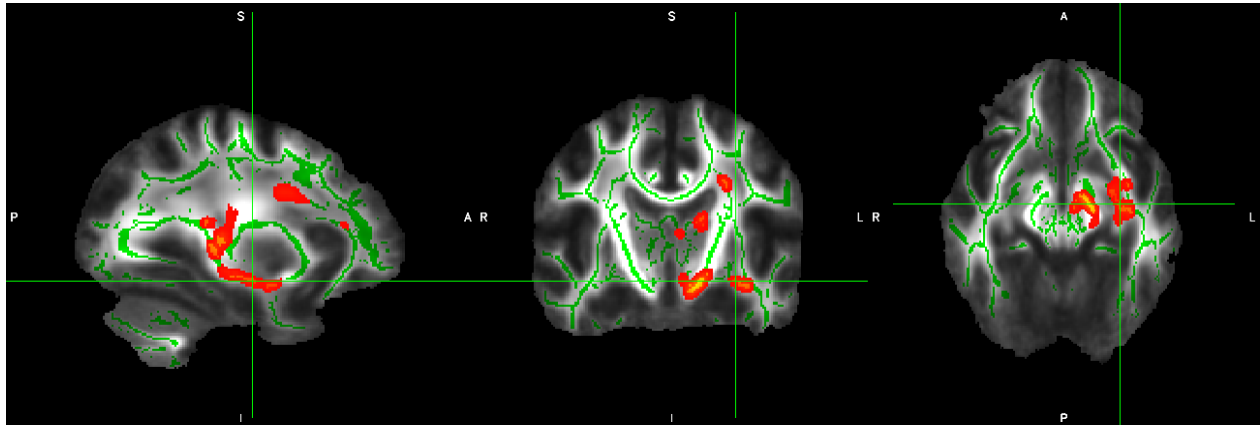


Figure 4. The average map of KFA and TBSS for right mTLE patients with three significant asymmetric clusters involving the underlying WM/subcortical GM of inferior, middle, and superior temporal gyri, inferior parietal lobule, hippocampus and parahippocampal gyrus, opercular part of inferior frontal gyrus, supramarginal gyrus, insula, thalamus, precentral and postcentral gyri, angular gyrus, fusiform gyrus, putamen, cingulum, cingulate gyrus, and insula. Note that the left side of the brains was flipped and overlaid on the right side and the normalized difference between them was calculated

comparison of our findings with previous studies might better reveal the nature of these asymmetries.

4.1. Interhemispheric Asymmetries in Left and Right mTLE

A bulk of evidence has demonstrated that structural and functional alterations in mTLE are mostly asymmetric [8, 30-32, 36]. Nonetheless, these reports are discrepant regarding the directionality, i.e. ipsilateral versus contralateral, of the changes. In this context, there are studies showing more diffuse and stark abnormalities in ipsilateral compared to contralateral hemisphere in mTLE [34, 37]. More specifically, while most studies have substantiated more bilateral and severe alterations in patients with left mTLE [7, 31, 33, 36], there are few reports of the contrary findings [38, 39]. Using connectometry approach on groups of mTLE and healthy controls [7], we have previously reported higher quantitative anisotropy for left ILF and forceps minor, but lower quantitative anisotropy for genu of Corpus Callosum (CC), bilateral Corticospinal Tract (CST),

and bilateral middle cerebellar peduncle (MCP) in right mTLE compared to controls. Left mTLE patients showed higher quantitative anisotropy for genu of CC, bilateral CSTs, and right MCP, but lower quantitative anisotropy for forceps minor, compared to controls. However, there are fewer studies of interhemispheric within each group of right and left mTLE.

In a recent TBSS study by Zhao *et al.* [34], it was demonstrated that mTLE-HS is associated with reductions of white matter microstructure asymmetry implying that innate interhemispheric asymmetry of the brain is compromised in mTLE. Interhemispheric asymmetries could be a double-edged sword; on the one hand, several studies suggest that structural and functional asymmetry is an advantageous characteristic of the healthy brain. In fact, it has been suggested that these asymmetries are in line with functional lateralization of brain functions, such as language, and are associated with better cognitive function of the brain [40-43]. On the other hand, it is evident that several brain diseases such as autism and epilepsy are associated with aberrant interhemispheric asymmetries [6, 44]. The differentiation between these normal or disease-related interhemispheric asymmetries could not be driven from the findings of the current study, it seems that left mTLE is associated with more reduced inherent side-to-side asymmetries in temporal region and more aberrant asymmetries in extra-temporal regions. Further studies with inclusion of healthy controls are required to investigate this suggestion.

4.2. Diffusion Kurtosis versus Diffusion Tensor Imaging

One of the main limitations of DTI is that it assumes the brain water diffusion as a Gaussian distribution

meaning that the brain is a bucket of water with no diffusion hindrance. This presumption makes DTI less ideal for the study of the brain, which is hindered with cell membranes and protein accumulations. As a corollary, DKI was developed as mathematical extension of DTI. Kurtosis is defined as a dimensionless index measuring the non-Gaussian distribution of water in a given voxel [45, 46] citing the voxel diffusional-hindered bucket of water. Unlike the FA, which can identify the diffusion restriction in an anisotropic environment, KFA is able to detect the restriction of diffusion in both isotropic and anisotropic environments [47]. Furthermore, it should be noted that FA and KFA quantify different properties of water diffusion and thus are associated with different sensitivities for identifying white matter alterations in regions with diverse microstructural characteristics. FA, which measures the mean directional diffusion anisotropy in a given voxel, is only appropriate for the assessment of the regions with coherent white matter fiber organization. Notwithstanding, it does not provide reliable information of water diffusion in voxels with complex (crossing or kissing) fiber orientations [48-50] as it averages the diffusion of all these crossing fibers into one direction. In contrast, KFA, which quantifies the non-Gaussian displacement probability distribution, is a more proper measure for the assessment of regions with complex fiber arrangements [51].

Our study is not the first one to compare the performance of DTI and DKI. In a recent study by Zhu *et al.* [5] in a group of patients with schizophrenia, it was demonstrated that altered diffusion measures were mostly resided in regions with coherent fiber orientation, including CC and Anterior Limb of Internal Capsule (ALIC), whereas altered kurtosis parameters were mainly located in regions with crossing fiber arrangement, including the juxtacortical white matter and Corona Radiata (CR). Herein, compared to FA findings of asymmetries, we found considerably more reduced interhemispheric asymmetries in patients with left mTLE when using KFA indicating that kurtosis parameters might be more sensitive measures of white matter asymmetries in patients with mTLE.

This study is not without limitations. First and foremost, the current study did not recruit healthy

controls. Inclusion of healthy controls could differentiate the inherent interhemispheric asymmetries in mTLE patients from those related to pathological processes. Secondly, we provided no assessment of cognitive functions in our sample. Thus, the cognitive implications of interhemispheric asymmetries should be elucidated in future studies.

5. Conclusion

In conclusion, extensive white matter interhemispheric asymmetries were found in the left and right mTLE patients using both DKI and conventional DTI. In comparison with conventional DTI, DKI could detect more decreased interhemispheric asymmetries only in patients with left mTLE. Besides, interhemispheric asymmetries were considerably different between patients with left and right mTLE. Left mTLE patients showed more extra-temporal asymmetries while right mTLE patients exhibited temporal asymmetries. Even so, compared to right mTLE, left mTLE patients demonstrated diminished overall interhemispheric asymmetries.

Our findings might have valuable implications for lateralization of seizure foci in clinical settings. However, further studies are required to investigate this issue.

Acknowledgements

We must acknowledge the contribution of Iranian National Brain Mapping Lab (NBML) and their staffs for MRI data acquisition throughout conducting this project.

References

- 1-R. Cabeza, "Hemispheric asymmetry reduction in older adults: the HAROLD model," (in eng), *Psychol Aging*, vol. 17, no. 1, pp. 85-100, Mar 2002.
- 2-S. Ocklenburg, P. Friedrich, O. Gunturkun, and E. Genç, "Intrahemispheric white matter asymmetries: the missing link between brain structure and functional lateralization?," (in eng), *Rev Neurosci*, vol. 27, no. 5, pp. 465-80, Jul 1 2016.

- 3-H. Takao, N. Hayashi, and K. Ohtomo, "White matter asymmetry in healthy individuals: a diffusion tensor imaging study using tract-based spatial statistics," (in eng), *Neuroscience*, vol. 193, pp. 291-9, Oct 13 2011.
- 4-A. W. Toga and P. M. Thompson, "Mapping brain asymmetry," *Nature Reviews Neuroscience*, vol. 4, no. 1, pp. 37-48, 2003/01/01 2003.
- 5-J. Zhu *et al.*, "Performances of diffusion kurtosis imaging and diffusion tensor imaging in detecting white matter abnormality in schizophrenia," (in eng), *Neuroimage Clin*, vol. 7, pp. 170-6, 2015.
- 6-R. A. Carper, J. M. Treiber, S. Y. DeJesus, and R. A. Muller, "Reduced Hemispheric Asymmetry of White Matter Microstructure in Autism Spectrum Disorder," (in eng), *J Am Acad Child Adolesc Psychiatry*, vol. 55, no. 12, pp. 1073-1080, Dec 2016.
- 7-H. Sanjari Moghaddam, F. Rahmani, M. H. Aarabi, M. R. Nazem-Zadeh, E. Davoodi-Bojd, and H. Soltanian-Zadeh, "White matter microstructural differences between right and left mesial temporal lobe epilepsy," (in eng), *Acta Neurol Belg*, Jan 11 2019.
- 8-M. E. Ahmadi *et al.*, "Side matters: diffusion tensor imaging tractography in left and right temporal lobe epilepsy," (in eng), *AJNR Am J Neuroradiol*, vol. 30, no. 9, pp. 1740-7, Oct 2009.
- 9-P. Besson *et al.*, "Structural connectivity differences in left and right temporal lobe epilepsy," (in eng), *Neuroimage*, vol. 100, pp. 135-44, Oct 15 2014.
- 10-H. J. Jo *et al.*, "Relationship Between Seizure Frequency and Functional Abnormalities in Limbic Network of Medial Temporal Lobe Epilepsy," (in English), *Original Research* vol. 10, no. 488, 2019-May-08 2019.
- 11-A. Lemkaddem *et al.*, "Connectivity and tissue microstructural alterations in right and left temporal lobe epilepsy revealed by diffusion spectrum imaging," *NeuroImage: Clinical*, vol. 5, pp. 349-358, 2014/01/01/ 2014.
- 12-J. Engel, Jr., "Introduction to temporal lobe epilepsy," (in eng), *Epilepsy Res*, vol. 26, no. 1, pp. 141-50, Dec 1996.
- 13-M. Catani, R. J. Howard, S. Pajevic, and D. K. Jones, "Virtual in vivo interactive dissection of white matter fasciculi in the human brain," (in eng), *Neuroimage*, vol. 17, no. 1, pp. 77-94, Sep 2002.
- 14-S. Mori *et al.*, "Imaging cortical association tracts in the human brain using diffusion-tensor-based axonal tracking," (in eng), *Magn Reson Med*, vol. 47, no. 2, pp. 215-23, Feb 2002.
- 15-M.-R. Nazem-Zadeh *et al.*, "DTI-based Response-Driven Modeling of mTLE Laterality " *NeuroImage Clinical*, 2015.
- 16-M. R. Nazem-Zadeh, J. M. Schwalb, K. V. Elisevich, H. Bagher-Ebadian, and H. Soltanian-Zadeh, "Lateralization of Temporal Lobe Epilepsy using a Novel Uncertainty Analysis of MR Diffusion in Hippocampus, Cingulum, and Fornix, and Hippocampal Volume and FLAIR Intensity," presented at the Gordon Research Conference on Mechanisms of Epilepsy & Neural Synchronization, West Dover, VT, USA, 2014.
- 17-M. R. Nazem-Zadeh, J. M. Schwalb, K. V. Elisevich, H. Bagher-Ebadian, and H. Soltanian-Zadeh, "Lateralization of Temporal Lobe Epilepsy by Analysis of Asymmetric Fractional Anisotropy in the Cingulum," presented at the 67th Annual Meeting of the American Epilepsy Society (AES), Washington, DC, USA, 2013.
- 18-P. J. Basser and D. K. Jones, "Diffusion-tensor MRI: theory, experimental design and data analysis - a technical review," (in eng), *NMR Biomed*, vol. 15, no. 7-8, pp. 456-67, Nov-Dec 2002.
- 19-D. S. Tuch, T. G. Reese, M. R. Wiegell, and V. J. Wedeen, "Diffusion MRI of complex neural architecture," (in eng), *Neuron*, vol. 40, no. 5, pp. 885-95, Dec 4 2003.
- 20-E. S. Hui, M. M. Cheung, L. Qi, and E. X. Wu, "Towards better MR characterization of neural tissues using directional diffusion kurtosis analysis," (in eng), *Neuroimage*, vol. 42, no. 1, pp. 122-34, Aug 1 2008.
- 21-H. Lu, J. H. Jensen, A. Ramani, and J. A. Helpert, "Three-dimensional characterization of non-gaussian water diffusion in humans using diffusion kurtosis imaging," (in eng), *NMR Biomed*, vol. 19, no. 2, pp. 236-47, Apr 2006.
- 22-V. Adisetiyo *et al.*, "Attention-deficit/hyperactivity disorder without comorbidity is associated with distinct atypical patterns of cerebral microstructural development," (in eng), *Hum Brain Mapp*, vol. 35, no. 5, pp. 2148-62, May 2014.
- 23-I. Blockx *et al.*, "Identification and characterization of Huntington related pathology: an in vivo DKI imaging study," (in eng), *Neuroimage*, vol. 63, no. 2, pp. 653-62, Nov 1 2012.
- 24-M. F. Falangola *et al.*, "Age-related non-Gaussian diffusion patterns in the prefrontal brain," (in eng), *J Magn Reson Imaging*, vol. 28, no. 6, pp. 1345-50, Dec 2008.
- 25-E. J. Grossman *et al.*, "Thalamus and cognitive impairment in mild traumatic brain injury: a diffusional kurtosis imaging study," (in eng), *J Neurotrauma*, vol. 29, no. 13, pp. 2318-27, Sep 2012.

- 26-S. Van Cauter *et al.*, "Gliomas: diffusion kurtosis MR imaging in grading," (in eng), *Radiology*, vol. 263, no. 2, pp. 492-501, May 2012.
- 27-S. M. Smith *et al.*, "Advances in functional and structural MR image analysis and implementation as FSL," *Neuroimage*, vol. 23, pp. S208-S219, 2004.
- 28-C. H. Chapman, M. R. Nazem-Zadeh, T. S. Lawrence, C. I. Tsien, and Y. Cao, "Regional variation in white matter diffusion index changes following chemoradiotherapy: A prospective study using tract-based spatial statistics," *Submitted to PLOS ONE*, 2012.
- 29-S. M. Smith *et al.*, "Tract-based spatial statistics: voxelwise analysis of multi-subject diffusion data," *Neuroimage*, vol. 31, no. 4, pp. 1487-1505, 2006.
- 30-A. Ashraf-Ganjouei *et al.*, "White matter correlates of disease duration in patients with temporal lobe epilepsy: updated review of literature," *Neurological Sciences*, vol. 40, no. 6, pp. 1209-1216, 2019/06/01 2019.
- 31-B. M. de Campos, A. C. Coan, C. Lin Yasuda, R. F. Casseb, and F. Cendes, "Large-scale brain networks are distinctly affected in right and left mesial temporal lobe epilepsy," (in eng), *Hum Brain Mapp*, vol. 37, no. 9, pp. 3137-52, Sep 2016.
- 32-Z. Haneef, A. Lenartowicz, H. J. Yeh, H. S. Levin, J. Engel, Jr., and J. M. Stern, "Functional connectivity of hippocampal networks in temporal lobe epilepsy," (in eng), *Epilepsia*, vol. 55, no. 1, pp. 137-45, Jan 2014.
- 33-F. R. Pereira *et al.*, "Asymmetrical hippocampal connectivity in mesial temporal lobe epilepsy: evidence from resting state fMRI," (in eng), *BMC Neurosci*, vol. 11, p. 66, Jun 2 2010.
- 34-X. Zhao *et al.*, "Reduced Interhemispheric White Matter Asymmetries in Medial Temporal Lobe Epilepsy With Hippocampal Sclerosis," (in English), Original Research vol. 10, no. 394, 2019-April-24 2019.
- 35-A. Arab, A. Wojna-Pelczar, A. Khairnar, N. Szabo, and J. Ruda-Kucerova, "Principles of diffusion kurtosis imaging and its role in early diagnosis of neurodegenerative disorders," (in eng), *Brain Res Bull*, vol. 139, pp. 91-98, May 2018.
- 36-N. Kemmotsu *et al.*, "MRI analysis in temporal lobe epilepsy: cortical thinning and white matter disruptions are related to side of seizure onset," (in eng), *Epilepsia*, vol. 52, no. 12, pp. 2257-66, Dec 2011.
- 37-W. M. Otte, P. van Eijsden, J. W. Sander, J. S. Duncan, R. M. Dijkhuizen, and K. P. Braun, "A meta-analysis of white matter changes in temporal lobe epilepsy as studied with diffusion tensor imaging," (in eng), *Epilepsia*, vol. 53, no. 4, pp. 659-67, Apr 2012.
- 38-M. Pail, M. Brazdil, R. Marecek, and M. Mikl, "An optimized voxel-based morphometric study of gray matter changes in patients with left-sided and right-sided mesial temporal lobe epilepsy and hippocampal sclerosis (MTLE/HS)," (in eng), *Epilepsia*, vol. 51, no. 4, pp. 511-8, Apr 2010.
- 39-N. L. Voets, C. F. Beckmann, D. M. Cole, S. Hong, A. Bernasconi, and N. Bernasconi, "Structural substrates for resting network disruption in temporal lobe epilepsy," (in eng), *Brain*, vol. 135, no. Pt 8, pp. 2350-7, Aug 2012.
- 40-V. Duboc, P. Dufourcq, P. Blader, and M. Roussigne, "Asymmetry of the Brain: Development and Implications," (in eng), *Annu Rev Genet*, vol. 49, pp. 647-72, 2015.
- 41-S. J. Gotts, H. J. Jo, G. L. Wallace, Z. S. Saad, R. W. Cox, and A. Martin, "Two distinct forms of functional lateralization in the human brain," (in eng), *Proc Natl Acad Sci U S A*, vol. 110, no. 36, pp. E3435-44, Sep 3 2013.
- 42-A. W. Toga and P. M. Thompson, "Mapping brain asymmetry," (in eng), *Nat Rev Neurosci*, vol. 4, no. 1, pp. 37-48, Jan 2003.
- 43-X. Yin *et al.*, "Inferior frontal white matter asymmetry correlates with executive control of attention," (in eng), *Hum Brain Mapp*, vol. 34, no. 4, pp. 796-813, Apr 2013.
- 44-W. Cao *et al.*, "Abnormal asymmetry in benign epilepsy with unilateral and bilateral centrotemporal spikes: A combined fMRI and DTI study," (in eng), *Epilepsy Res*, vol. 135, pp. 56-63, Sep 2017.
- 45-J. H. Jensen and J. A. Helpern, "MRI quantification of non-Gaussian water diffusion by kurtosis analysis," vol. 23, no. 7, pp. 698-710, 2010.
- 46-J. H. Jensen, J. A. Helpern, A. Ramani, H. Lu, and K. Kaczynski, "Diffusional kurtosis imaging: The quantification of non-gaussian water diffusion by means of magnetic resonance imaging," vol. 53, no. 6, pp. 1432-1440, 2005.
- 47-A. J. Steven, J. Zhuo, and E. R. Melhem, "Diffusion kurtosis imaging: an emerging technique for evaluating the microstructural environment of the brain," (in eng), *AJR Am J Roentgenol*, vol. 202, no. 1, pp. W26-33, Jan 2014.
- 48-G. Douaud *et al.*, "DTI measures in crossing-fibre areas: increased diffusion anisotropy reveals early white matter alteration in MCI and mild Alzheimer's disease," (in eng), *Neuroimage*, vol. 55, no. 3, pp. 880-90, Apr 1 2011.
- 49-S. Jbabdi, T. E. Behrens, and S. M. Smith, "Crossing fibres in tract-based spatial statistics," (in eng), *Neuroimage*, vol. 49, no. 1, pp. 249-56, Jan 1 2010.

50-S. B. Vos, D. K. Jones, B. Jeurissen, M. A. Viergever, and A. Leemans, "The influence of complex white matter architecture on the mean diffusivity in diffusion tensor MRI of the human brain," (in eng), *Neuroimage*, vol. 59, no. 3, pp. 2208-16, Feb 1 2012.

51-M. Lazar, J. H. Jensen, L. Xuan, and J. A. Helpert, "Estimation of the orientation distribution function from diffusional kurtosis imaging," (in eng), *Magn Reson Med*, vol. 60, no. 4, pp. 774-81, Oct 2008.